Available online at www.sciencedirect.com
ScienceDirect
Combustion and Flame 151 (2007) 235–244
Combustion and Flame
www.elsevier.com/locate/combustflame

Effect of ethanol on the chemical structure of the soot extractable material of an ethylene inverse diffusion flame

Alexander Santamaría [a], Eric G. Eddings [b], Fanor Mondragón [a,*]

[a] *Institute of Chemistry, University of Antioquia, A.A. 1226, Medellín, Colombia*
[b] *Department of Chemical Engineering, University of Utah, Salt Lake City, UT 84112, USA*

Received 26 October 2006; received in revised form 1 June 2007; accepted 15 June 2007

Available online 26 July 2007

Abstract

The effect of fuel-side ethanol addition on the chemical structure of the soot extractable material generated in an ethylene inverse diffusion flame was evaluated by means of average structural parameters. The results indicate that the ethanol effect on the aromatic components was more pronounced, with an increase of about 40% in the average number of aromatic fused rings (R_a) as compared to the results of a neat flame. This observation also helps explain the low percentage of chloroform-extractable material in the soot samples obtained from the flame with ethanol addition. In contrast, the aliphatic component of the extractable material did not demonstrate significant changes with ethanol addition.

Keywords: Soot precursors; Ethanol effect; Inverse diffusion flame; Average structural parameters; Aromatization

1. Introduction

Incomplete combustion of fossil fuels leads to soot formation, which is in many cases an unwanted product, not only because it can affect the correct functioning of combustion devices, but also because its emission into the environment can have serious consequences for human health due to the large amount of polyaromatic hydrocarbons adsorbed onto the surface of theses particles [1,2]. Therefore, the health risks associated with these compounds are not only mutagenic, but also potentially carcinogenic. As a result, government agencies have introduced strict control measures that regulate the emission of soot particles into the environment [3–5].

An approach that has been widely used to control the emission of particulate matter (PM) into the environment is the use of fuel additives [6–23]. However, the role of additives in the reduction of PM is still unclear at a molecular level. For example, it has been found that some additives can inhibit some stages of soot formation, while in other cases; they can act as catalysts to enhance the soot oxidation process [6–10].

The vast majority of additives known so far can be classified into two categories, metallic additives and oxygenated compounds [6–23]. Previous studies have shown that the addition of some alkali or alkaline-earth metals (Na, Li, Mg, K) can cause an increase in the number of particles with a decrease in the soot particle size [6–9]. Haynes and co-workers suggested

* Corresponding author. Fax: +574 210 6565.
E-mail address: fmondra@quimbaya.udea.edu.co (F. Mondragón).

0010-2180/$ – see front matter
doi:10.1016/j.combustflame.2007.06.004

that alkali metal ions transfer their charge to young soot particles, resulting in the inhibition of the coagulation and coalescence processes due to the presence of electrostatic repulsion [7,8].

In studies carried out in methane diffusion flames doped with ferrocene $(C_2H_5)_2Fe$, it was found that the number of particles is reduced by an increase in the oxidation rate rather than by the inhibition of the processes leading to the soot formation, since this leads to the formation of condensation nuclei (iron oxide nuclei) in the combustion zone that serve as a seed for carbonaceous matter deposition, which is burned more effectively in the last stage of the combustion process [9–12]. Similar results obtained in ethylene diffusion flames have shown that iron oxide incorporated into the soot particles can act as a catalyst to promote the conversion of soot in the flame oxidation zone [9,12,13].

Although many metallic additives have shown high efficiency in the soot reduction process, unfortunately their use has been limited due to concerns about adverse human health and environmental impacts, as well as incompatibility with gas turbine engines [10,20,21].

An alternate additive proposed in recent years for use in combustion systems is based on the incorporation of oxygenated compounds (e.g., acetals and alcohols) [17–23]. These compounds can play a dual role: on one hand, the pyrolytically formed fragments emanating from oxygenated compounds increase the formation of soot precursors; on the other hand, these additives open a more direct route to the formation of products such as H_2CO, HCO, and CO, which no longer take part in the soot formation process [20–23].

It is important to mention that oxygenated compounds may not be the ultimate solution to the problem of particulate matter emissions from combustion systems, since these additives need to be added in relatively high concentrations to have a noticeable effect, which makes them impractical in some cases [20,21].

Previous studies have demonstrated that the use of additives in combustion systems can have a considerable effect on the flame structure, temperature, and formation of radicals and combustion products such as soot and polycyclic aromatic hydrocarbons. This effect may be different depending on whether the additive is mixed with the fuel or the oxidizer stream [14,21]. For example, when iron pentacarbonyl ($Fe(CO)_5$) is added to the air streams of many opposed diffusion flames, the reduction of soot is quite significant; however, when the additive is introduced on the fuel side, this effect is less pronounced [14].

Recent studies in ethylene premixed flames using ethanol as an additive have shown that the amount of aromatic species formed is reduced due to the removal of the carbon available for the formation of molecular precursors through reaction pathways that lead to an increase in CO production [20]. In contrast, ethanol addition to the fuel stream of opposed-flow diffusion flames was found to increase the aromatic species formation, due to an increase in the C4 species concentration, which then reacts with the acetylene pool to form benzene and subsequently, PAHs [21]. Unfortunately, this difference in behavior is not well documented in the literature.

To study the effect of additives on the chemical structure of young soot precursor material, the inverse diffusion flame configuration (IDF) has been chosen as a good alternative since it provides certain advantages as compared to normal diffusion flames, such as (1) the IDF provides a better separation of oxidation and pyrolysis processes, (2) it is possible to collect a significant amount of young soot without the need to invade the flame with the sampling probe, and (3) more than 50% of the soot is chloroform-extractable material, which allows a direct chemical analysis of the sample using different analytical techniques [24–30].

The purpose of this work was to evaluate the effect of fuel-side ethanol addition on the chemical structure of the soot precursor material generated in an ethylene inverse diffusion flame. To carry out this effort, average structural parameters obtained from ^1H NMR, vapor pressure osmometry (VPO), and elemental analysis data were used. A detailed discussion of each of these parameters is found in Ref. [30].

2. Experimental methods

2.1. Burner and fuel additive

The IDF burner used in this study consists of three concentric brass tubes: a central tube or air jet, an intermediate tube used to supply the ethylene, and an outer tube that conveys a N_2 stream, which is used as a shield to prevent the formation of flames with room air. The flow conditions for the gaseous system were set to 27, 117, and 289 cm^3/s for air, fuel and N_2, respectively (see Fig. 1).

The additive was introduced into the reaction system at room temperature by bubbling the fuel through absolute ethanol at the flow rate specified above. By this procedure, 4% by mass of ethanol was mixed with the fuel stream.

2.2. Sampling procedure

The soot samples were taken at different heights along the lateral axis at a radial position of 6 mm,

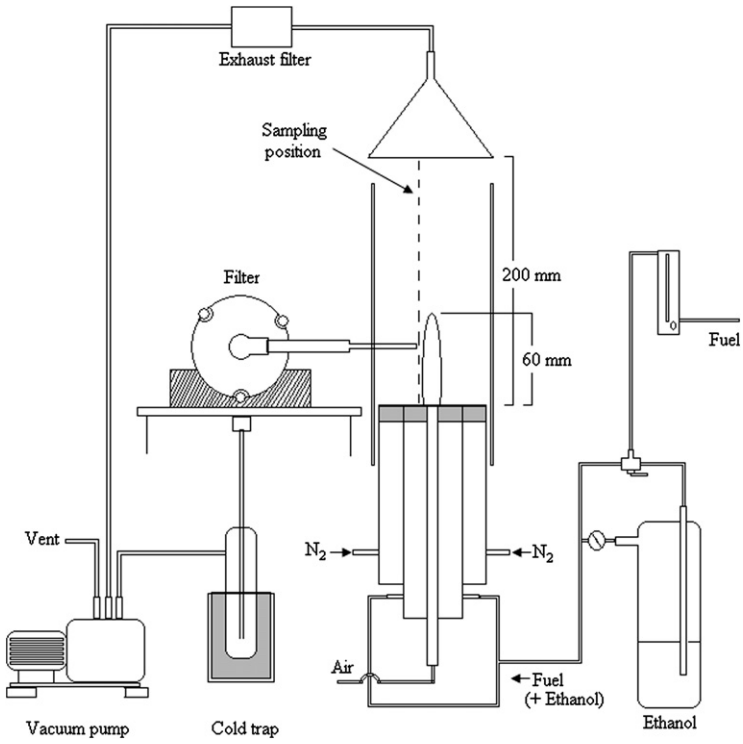

Fig. 1. Experimental setup of an ethylene IDF with and without ethanol.

using a 10-cm-long stainless steel probe with a capillary tip of 1 mm. The sampling time for each experiment depended on the amount of sample that could be collected on the filter, which was different at each position of the flame and varied from 20 min to 1 h. The sampling rate was adjusted at 400 ml/min, which causes no apparent perturbation of the flame structure. The filter temperature was about 40 °C in all cases. The sample retained on the filter and sampling probe was washed and extracted with chloroform in an ultrasonic bath for 15 min. Then the soluble and insoluble fractions were separated and the extracted material was placed in an oven at 60 °C under inert conditions in order to evaporate the solvent.

2.3. Flame temperature

The temperature profiles along the lateral axis of the flame (sampling position) were obtained using an R-type thermocouple (Pt–Pt 13% Rh, 75 μm, with a bead diameter of about 150 μm), which was placed in the flame by a rapid insertion method in order to reduce the exposure time of the thermocouple in the sooting region. Radiation corrections of the thermocouple readings were taken into account to calculate the gas temperature at each location.

2.4. Characterization methods

^{1}H NMR spectra were taken in a Bruker AMX 300 spectrometer operated at 300 MHz. The extracts of the soot samples were redissolved in $CDCl_3$ with traces of tetramethylsilane (TMS), which was used as chemical shift reference. Later, each spectrum was divided into seven regions that correspond to seven different types of protons: aromatic hydrogen (H_a, 6.0–9.0 ppm), olefinic hydrogen (H_o, 4.5–6.0 ppm), flourene-type hydrogen (H_f, 3.7–4.5 ppm), hydrogen on α carbons to aromatic rings (H_α, 2.0–3.7 ppm), hydrogen on $\beta 2$ carbons to aromatic rings, mainly CH_2 or naphthenic-type carbon ($H_{\beta 2}$, 1.4–2.0 ppm), hydrogen on $\beta 1$ carbons to aromatic rings ($H_{\beta 1}$, 1.0–1.4 ppm), and hydrogen on γ carbons or CH_3 terminal of aliphatic chains alkylating an aromatic ring (H_γ, 0.5–1.0 ppm). The integration of the spectra was carried out manually, a minimum of four times, and the results were averaged to reduce the uncertainty (less than 5%) generated by the manual adjustment.

Elemental analysis of the soot extracts was carried out by the combustion method using a Perkin–Elmer CHN analyzer. Hydrogen and carbon were determined directly, while the oxygen content present in the samples was calculated by difference, assuming a base of 100%. These experiments were repeated three times per sample and the reproducibility was quite

Table 1
Calculation of average structural parameters

$$f_a = \frac{[C^* - (0.33H^*_\gamma + 0.4H^*_{\beta 1} + 0.5(H^*_{\beta 2} + H^*_\alpha + H^*_f) + H^*_o + C^*_q)]}{C^*} \quad (1)$$

$$f_{al} = \frac{[(0.33H^*_\gamma + 0.4H^*_{\beta 1} + 0.5(H^*_{\beta 2} + H^*_\alpha + H^*_f))]}{C^*} \quad (2)$$

$$f_\alpha = \frac{[0.5H^*_\alpha]}{C^*} \quad (3)$$

$$f_{aH_a} = \frac{H^*_a}{C^*} \quad (4)$$

$$\%C_i = f_i(\%C),\ i = \mathrm{a}, \mathrm{al}, \alpha, \mathrm{f}, \ldots \quad (5)$$

$$\#C_i = (\%C_i)\mathrm{MW}/1200,\ i = \mathrm{a}, \mathrm{al}, \alpha, \mathrm{f}, \ldots \quad (6)$$

$$L = (\#C_{al} - \#C_f)/\#C_\alpha \quad (7)$$

$$R_a = 1 + (\#C_a - \#C^s_a)/2 \quad (8)$$

good, since the estimated error was less than 2% in all cases.

The average molecular weight data (MW) of the soot extracts were determined by vapor pressure osmometry (VPO) in a Knauer osmometer using chloroform as solvent and benzyl as standard of calibration. Then the molecular weight was obtained from the K_{cal}/K_s ratio, where K_{cal} is the calibration constant for benzyl expressed in kg/mol and K_s is the value measured for the sample, which is expressed in kg/g.

3. Average structural parameters

The methodology and the equations involved in the calculations described below have been used extensively to describe the chemical and structural characteristics of coal and oil soluble fractions [31–33]. However, this is the first time that this methodology has been used to characterize soot precursor material. In this study, the average structural parameter calculation was based on the data obtained by elemental analysis, ^{1}H NMR, and average molecular weight. A detailed description of the method can be found in Ref. [30]; however, a brief description is given here. Table 1 shows the equations used to calculate some of the parameters evaluated in this study. The variables labeled as H^*_α, $H^*_{\beta 1}$, $H^*_{\beta 2}$, H^*_γ, H^*_o, H^*_f, and H^*_a correspond to the molar fractions of the different types of hydrogen obtained from the integral of the normalized signals of each spectra. Variables such as C^*, H^*, and MW correspond to the molar fraction of carbon, hydrogen, and average molecular weight obtained directly by elemental analysis and VPO.

The parameters f_a, f_{al}, f_α, and f_{aH_a} correspond to the carbon fractions on aromatic and aliphatic structures, carbons in α position to aromatic rings, and protonated aromatic carbons, respectively. The weight percentage of carbons ($\%C_i$) and the average number of carbons ($\#C_i$) related to the different hydrogen groups ($i = \mathrm{a}, \mathrm{al}, \mathrm{f}, \alpha, \ldots$) are obtained from Eqs. (5) and (6) of Table 1.

Similarly, parameters that correspond to the average chain length of aliphatic structures (L) and average number of fused aromatic rings (R_a) were included in this analysis through Eqs. (7) and (8), respectively. Note that the variable $\#C^s_a$ in Eq. (8), corresponds to the total number of substituted aromatic carbons; not only for aromatic hydrogen, but also for other functional groups such as aliphatic chains and oxygenated species.

The precision of this method was estimated by carrying out three replicas on a pair of samples; as a result, parameters such as f_a and R_a showed an error below 5%, f_{aH_a} and f_{al} showed an error between 5 and 10%, whereas f_α and L showed an estimated error between 10 and 20%. Similarly, parameters derived from the quantities described above, such as $\%C_i$ and $\#C_i$ (where $i = \mathrm{a}, \mathrm{al}, \alpha, \mathrm{f}, \ldots$), also fall within the estimated error for each category. It is worthwhile to note that the oxygen content present in these samples has been incorporated into the calculation, with the assumption that 50% is distributed in oxygenated species of the quinone type (O_q), which is equivalent to the content of carbonyl carbons (C_q). On the other hand, according to the FT-IR analysis previously published, the remaining 50% of the oxygen is designated as oxygenated species of the ether type [29,34,35].

4. Results and discussion

Fig. 2 shows the temperature profiles along the lateral axis of the flame with and without ethanol. The profile with open squares corresponds to the neat flame temperature, whereas the profile with the enclosed circles corresponds to the doped flame with 4% ethanol. Both profiles have similar behavior as the height above the burner increases. Note that the temperature is kept above 1200 K during the first 25 mm, with the highest temperature peak centered at about 15 mm, after which the temperature decreases to 800 K at a height equal to the tip of the flame.

Although the differences in temperature between the two cases are not very significant, the overall trend would indicate that the temperature profile of the doped flame is lower than that of the neat flame, since the former requires more energy to heat up not only the fuel but also the ethanol added. McNesby

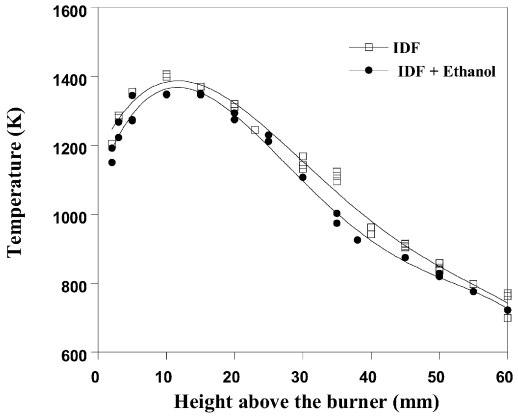

Fig. 2. Temperature profiles of an ethylene IDF with and without ethanol.

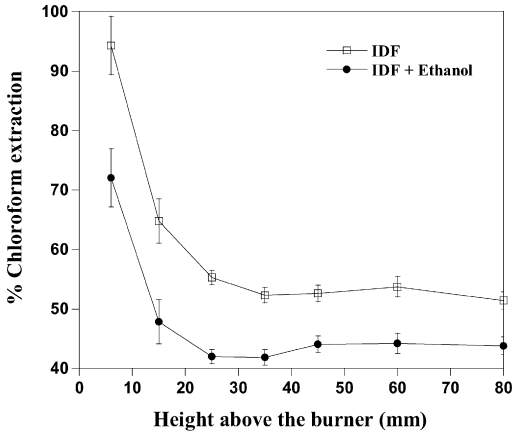

Fig. 3. Weight percentage of chloroform extractable material of the soot collected from an ethylene IDF with and without ethanol.

et al. [21], using an ethylene opposed-flow diffusion flame (a configuration somewhat similar to the IDF used here), did not find important changes in the temperature due to fuel-side ethanol addition, nor did they observe changes in the OH radical concentration, which suggests that the process that governs this type of situation (fuel + ethanol) may be the pyrolysis step rather than oxidation.

Fig. 3 shows the variation in the weight percentage of the soot extractable material as a function of height above the burner for both cases: with and without ethanol addition. In general, the amount of extractable material decreases considerably during the first 25 mm, independent of the ethanol addition. After this point, the samples of each series reach a constant value, suggesting that the chemical composition of soot may have similar patterns. The reproducibility of each result was carried out on several samples (from 7 to 10) and the error associated with these

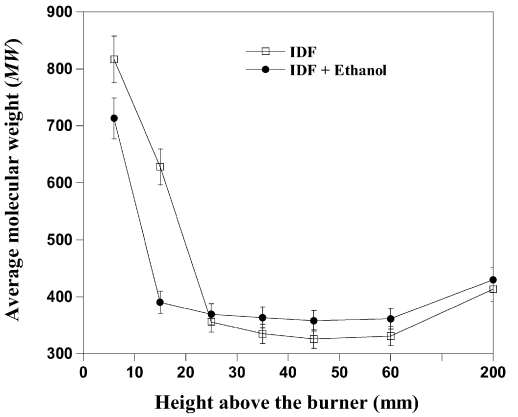

Fig. 4. Average molecular weight (MW) of soot extractable material gathered from an ethylene IDF with and without ethanol addition.

measurements was below 5% (noted by the error bars in Fig. 3).

Fig. 3 also shows that the effect of ethanol addition on the fuel side is reflected in a marked reduction of the extractable material in chloroform. For example, the amount of extractable material in the soot sample taken at a 6-mm height in the flame without additive is approximately 95%, whereas the amount of extractable material of the soot taken at the same height for the doped flame diminishes 24%. A similar difference is observed with the soot sample taken at 15 mm, where a variation of about 26% in the chloroform-extractable material is observed. However, for the rest of samples, the reduction in the amount of extractable material due to the ethanol effect varies between 15 and 19%. The decrease in the amount of the soot extractable material in chloroform due to ethanol addition is mainly caused by an increase in the aromaticity of the samples, which leads to the formation of more compact structures with a large number of fused aromatic rings as will be shown later.

A similar trend is obtained when we analyzed the average-molecular-weight information for the extracts, as shown in Fig. 4. Notice that the average molecular weight is larger for the samples taken near the burner base. However, comparing the two series, the effect of the ethanol addition is reflected in a reduction of the average molecular weight of these samples early on in the flame. For example, the average molecular weight of the samples taken at 6 mm is reduced from 817 to 713 Da when the ethanol effect is considered. However, variations in the average molecular weight of the samples after 25 mm is not very important and they reach a constant value of about 370 Da, which indicates that after this point the ethanol addition does not have a significant effect on the molecular weight.

Table 2
Elemental analysis of the extractable material of soot gathered from an ethylene IDF with and without ethanol

Height (mm)	%C		%H		%O		(C/H) total	
	A	B	A	B	A	B	A	B
6.0	85.3	86.2	7.71	7.69	7.02	6.11	0.92	0.93
15.0	86.5	91.7	6.42	5.77	7.12	2.49	1.12	1.32
25.0	88.9	92.2	5.44	5.47	5.67	2.36	1.36	1.40
35.0	90.2	92.7	4.90	4.98	4.90	2.37	1.53	1.55
45.0	92.9	93.4	4.89	5.03	2.21	1.56	1.58	1.55
60.0	93.6	93.7	5.24	4.93	1.12	1.37	1.49	1.58
Exhaust	93.7	94.0	5.20	4.84	1.12	1.16	1.50	1.62

Note. A = soot extractable material gathered from an ethylene IDF. B = soot extractable material gathered from an ethylene IDF + ethanol.

Table 2 summarizes the elemental analysis results of the soot extracts taken at different positions of the flame, which are basically composed of C, H, and O. The labels A and B are used to distinguish the samples that were taken from the neat and doped ethylene flames, respectively. In general, the carbon content of the samples increases as height above the burner increases. In addition, when ethanol is added, the carbon content of the samples is higher than that obtained at the same position of the flame without ethanol. The difference is more marked in the first 25 mm, which is consistent with the trend in the solubility results.

The hydrogen content, on the other hand, showed behavior opposite to the carbon content, since it decreases as height above the burner increases. Therefore, the total C–H ratio of the soot extractable material increases from 0.92 at 6 mm high up to 1.62 at the exhaust, which suggests that the sample may be losing aliphatic structures.

The oxygen content also showed a pronounced tendency. For example, the sample taken at 6 mm of the neat flame shows the highest oxygen content (7.02). However, as the height above the burner increases, the oxygen content decreases to 1% in the sample taken at the exhaust. Something similar appears in the samples of the flame with ethanol, but in this case the oxygen content is reduced much more rapidly after 6 mm. Previous results indicate that the oxygen content present in these samples is assigned mainly to oxygenated species of the quinone and ether types [29,34,35].

^{1}H NMR spectra of the soot extracts taken at flame heights of 6, 15, and 60 mm and the exhaust of an ethylene inverse diffusion flame, with and without ethanol addition, are shown in Fig. 5. For convenience, the aliphatic and aromatic regions of each spectrum were enlarged and normalized to the same scale, allowing comparisons within the groups. The dotted line spectra correspond to the extractable material of soot samples of the neat flame, whereas the continuous line spectra correspond to the soot extractable material obtained from the doped flame.

In general, the spectra show that the aliphatic component of the samples decreases as the height increases, which is reflected in the reduction of hydrogens H_γ, $H_{\beta 1}$, and $H_{\beta 2}$, whereas the aromatic hydrogen content increases considerably, corroborating the increase in the degree of aromatization. However, the aromatic hydrogen content observed in the ethylene–ethanol flame is lower as compared to the base flame. This result may be indicative of two things: (1) a reduction in the number of small aromatic compounds, or (2) an increase of the number of fused aromatic rings. In this sense, both cases would explain the increase in the aromaticity and the reduction of the solubility of the samples. Moreover, only the second one would explain the increment of the carbon content observed by elemental analysis.

It is important to highlight that the ^{1}H NMR analysis gives us indirect information on the aromaticity. That is why it is necessary to use caution in the interpretation of the results obtained by this technique. Since an increment in the aromatic hydrogen content does not always imply an increment in the aromatic cluster content or vice versa, the analysis would not be complete without taking into account the carbon content.

Other characteristics can be observed when the ethanol effect is considered. For example, the fraction of hydrogen $H_{\beta 1}$ and $H_{\beta 2}$ is much more significant for the samples obtained at 60 mm and at the exhaust, which indicates that the average chain length must be a little longer for these samples compared with the samples obtained at the same position of the neat flame.

In the case of the aromatic region of the spectra, the aromatic content of the sample taken at 6 mm high has a hydrogen distribution between 6 and 7 ppm, which correspond to isolated mono- and diaromatic compounds. A similar distribution can be seen even in the sample obtained at 15 mm high, with the only difference that the contribution of aromatic species with more than two rings is much more significant.

Although the aromatic hydrogen content (H_a) for compounds with more than two aromatic rings in the sample obtained at 6 mm is less significant, this does not mean that these types of structures are absent. For example, the high total carbon content present in this sample (see Table 2) suggests the possibility of finding highly condensed structures with large numbers of fused carbons that are not possible to see by this technique. However, combining the ^{1}H NMR data with the data obtained by elemental analysis and average molecular weight, it is possible to obtain information on the number of fused aromatic carbons or average

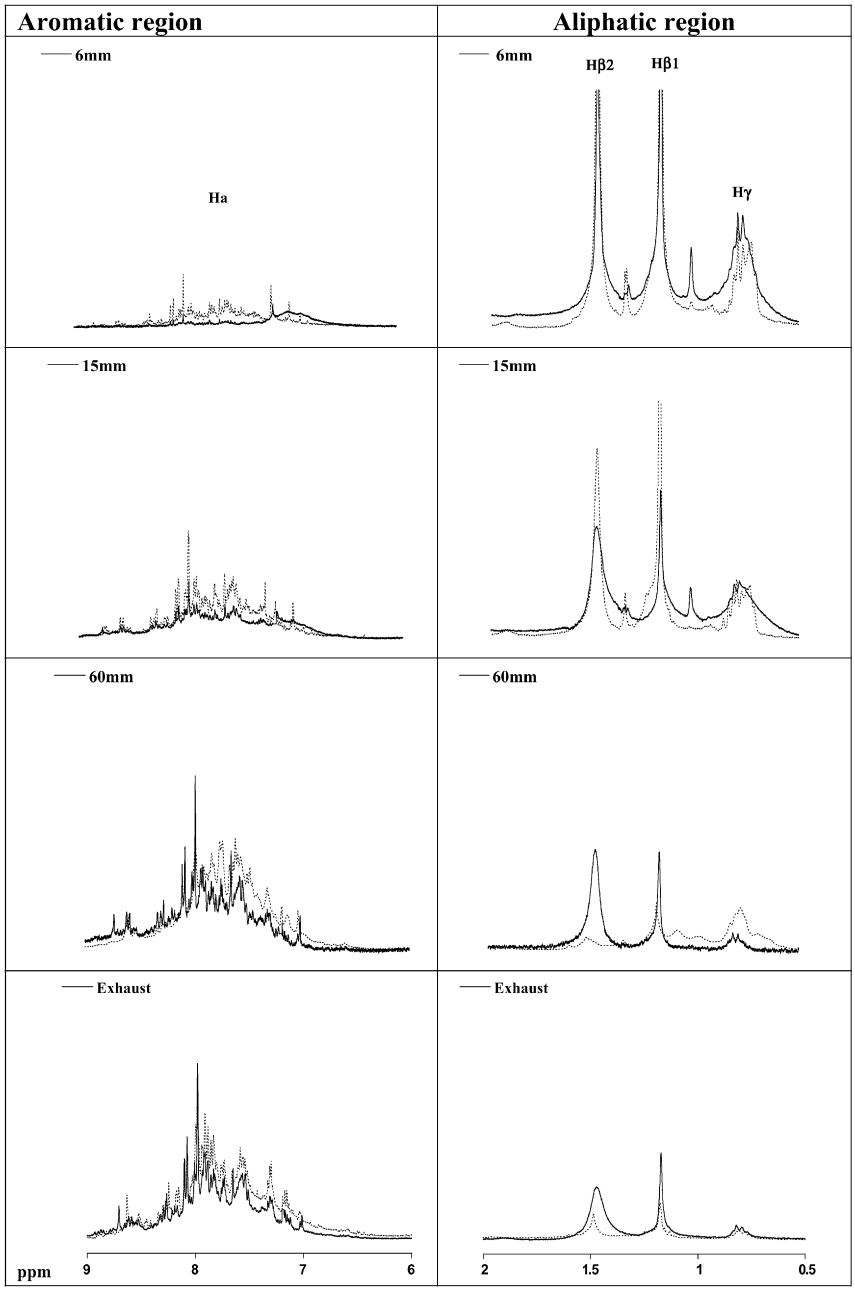

Fig. 5. ^{1}H NMR spectra of the soot extracts collected from an ethylene IDF as a function of height: (—) ethanol-doped flame and (···) neat flame.

number of fused aromatic rings, which will be explained in detail below.

The average structural parameter results evaluated in this study for the chloroform-soluble material of both neat and doped flame are summarized in Table 3. As can be observed, all the evaluated parameters change along the position in the flame. For example, the parameters associated with the aromatic carbon fraction (f_a) and the weight percent of aromatic carbons ($\%C_a$) increase as height above the burner increases, which indicates that the degree of aromatization also increases. However, no significant effect due to the ethanol addition was observed in these two parameters.

The sudden increase in $\%C_a$ observed from 6 to 15 mm, reflected in the total carbon content $\%C$ ob-

Table 3
Average structural parameters results of the extractable material of soot gathered from an ethylene IDF with and without ethanol situations

Height (mm)	Neat flame					Flame + 4% ethanol				
	6	15	35	60	Exhaust	6	15	35	60	Exhaust
f_a	0.59	0.75	0.89	0.95	0.96	0.57	0.79	0.89	0.93	0.94
f_{al}	0.34	0.20	0.08	0.05	0.04	0.37	0.19	0.11	0.07	0.05
f_α	0.06	0.04	0.01	0.01	0.01	0.06	0.03	0.02	0.01	0.01
f_{aH_a}	0.26	0.42	0.45	0.56	0.60	0.17	0.30	0.39	0.47	0.49
$f_a - f_{aH_a}$	0.33	0.33	0.44	0.39	0.36	0.40	0.49	0.50	0.46	0.45
$\%C_a$	49.9	64.5	80.4	88.9	89.5	49.5	72.1	82.2	86.8	88.6
$\%C_{al}$	29.3	16.9	7.24	4.26	3.73	31.9	17.8	9.78	6.48	5.07
$\%C_\alpha$	4.74	3.12	0.89	0.98	0.86	5.12	3.14	1.94	1.28	1.08
$\%C_{aH_a}$	21.8	36.1	40.9	52.6	55.9	14.9	27.7	36.6	44.2	46.5
$\#C_a$	34.0	33.7	22.4	24.5	30.8	29.4	23.5	24.9	26.1	30.8
$\#C_{al}$	19.9	8.86	2.02	1.18	1.29	18.9	5.78	2.96	1.95	1.77
$\#C_\alpha$	3.23	1.63	0.25	0.27	0.30	3.04	1.02	0.59	0.39	0.37
$\#C_{aH_a}$	14.9	18.9	11.4	14.5	19.2	8.86	9.00	11.1	13.3	16.2

tained by elemental analysis (Table 2), indicates that significant aromatization occurs much earlier in the doped flame than in the neat flame. This occurrence is favored by the temperature, which is high enough in this region.

Another important parameter that is related to f_a is the protonated aromatic carbon fraction (f_{aH_a}), which is obtained directly after integrating the aromatic hydrogen region in the resonance spectra. In general, f_{aH_a} increases in both situations as a function of height above the burner surface. However, comparing the two series, it is easy to note that the effect due to the ethanol addition is much more significant and it is reflected in the reduction of f_{aH_a}. For example, the f_{aH_a} fractions for the samples taken at a height of 6 mm in an ethylene flame with and without ethanol are 0.26 and 0.17, respectively. This result indicates that the size of aromatic structures must be larger in the flame with ethanol.

This characteristic can be also confirmed through the calculation of the fraction of fused aromatic carbons present in the samples. This parameter is estimated by subtracting f_{aH_a} from f_a. Results of this operation indicate that the fraction of fused aromatic carbons in rings is larger in the doped flame samples than in the neat flame. The same reasoning can be obtained using the parameter that corresponds to the number of protonated aromatic carbons ($\#C_{aH_a}$).

On the other hand, parameters that correspond to the alkyl component, such as the fraction of aliphatic carbons (f_{al}) and the fraction of α carbons joined to aromatic rings (f_α), decrease as a function of height above the burner in both cases. Nonetheless, these variables do not show significant changes due to the ethanol addition, a fact that can be corroborated through the parameters derived from f_{al} and f_α, such as $\%C_{al}$, $\#C_{al}$, $\%C_\alpha$, and $\#C_\alpha$.

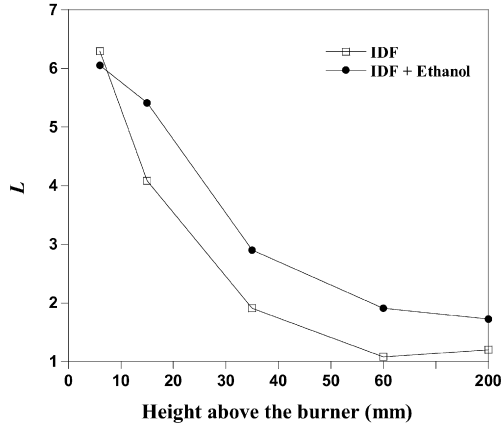

Fig. 6. Average aliphatic chain length (L) of the soot extracts gathered from an ethylene IDF with and without ethanol addition.

It is also important to mention that the $\#C_\alpha$ values reported in Table 3 are underestimated due to the high error associated with the calculation of f_α (approx 18%), since this fraction is quite variable in the ^{1}H NMR spectra of these samples. However, if we take into account that the number of aliphatic carbons, $\#C_{al}$, present in the samples taken above 25 mm is almost constant, we can assume that there is at least one α carbon atom per structural unit. Therefore, for a corrected $\#C_\alpha$ value, it is possible to estimate the average chain length (L) of the samples using Eq. (7).

Fig. 6 shows the average aliphatic chain length (L) of the soot-extractable material for both types of flames estimated by this methodology. Note that L decreases as a function of height mainly due to thermal decomposition processes that cause the bond scission of some aliphatic structures, particularly during the first 25 mm, where the temperature is still high. Also,

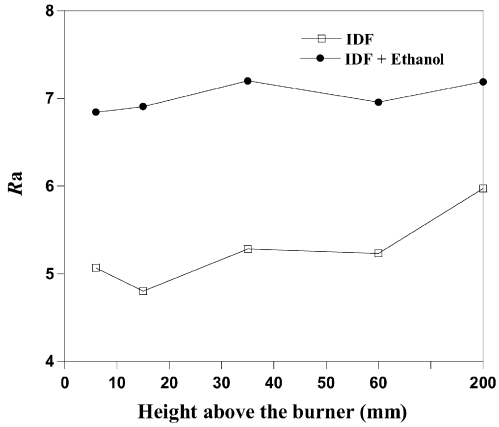

Fig. 7. Average number of fused aromatic rings (R_a) of the soot extracts gathered from an ethylene IDF with and without ethanol addition.

it is possible to observe the effect of ethanol addition on the value of L, and Fig. 6 indicates a slight increase in the value of L for heights above 15 mm.

Fig. 7 shows the variation in the number of fused aromatic rings number (R_a) for both conditions as a function of height. There is a considerable increase in R_a as a result of the ethanol addition, which yields values of approximately seven aromatic rings per cluster. In contrast, for the samples taken from the neat flame the number of fused aromatic rings is much lower, with values between five and six aromatic rings per cluster. This result also indicates that the aromatic clusters are formed rapidly in the flame, independent of the ethanol addition, which explains the high molecular weights observed lower in the flame (6 and 15 mm), where there are not only large aromatic clusters, but also a significant contribution of aliphatic and oxygenated species.

Unfortunately, with the information obtained thus far, it is not possible to delineate a plausible explanation for how these aromatic clusters can grow in the ethylene–ethanol flame, since it is necessary to take into account not only the chemical decomposition of ethanol, but also a detailed chemical analysis of the gas phase.

In summary, it has been shown that the addition of ethanol to ethylene inverse diffusion flames will change the nature of the aromatic components of the flame. A reduction of protonated aromatic carbons (f_{aH_a}, $\%C_{aH_a}$, and $\#C_{aH_a}$), along with an increase in the number of fused aromatic carbons, was observed. This result suggests that the aromatic cluster size found in the soot extractable material collected in the doped ethanol flame is larger and, therefore, this type of soot may have different environmental impacts as compared to the soot produced in a flame without ethanol addition.

5. Conclusions

The effect of fuel-side ethanol addition has been studied through the chemical structure of the extractable material of soot generated in an ethylene inverse diffusion flame. In general terms, both cases (with and without ethanol) demonstrate similar trends as height above the burner increases. Nevertheless, when ethanol is added to the flame, some notable changes can be observed. For example, the amount of chloroform-extractable material in the soot decreases significantly for both flames during the first 25 mm, but there is an additional reduction of 20 to 30% in the ethanol-doped flame as compared to the neat flame.

Similarly, the average molecular weight of the chloroform-soluble components obtained during the first 25 mm is reduced to almost half of the value obtained at the base of the burner, independent of the ethanol addition. This reduction in molecular weight is mainly caused by fragmentation of the aliphatic structures that are formed in the early stages of the flame, leaving behind a well-defined aromatic cluster that remains constant in size after 25 mm.

The reduction in molecular weight observed during the first 25 mm is accompanied by an increase in the aromatic character of the samples, as described through the structural parameters f_a, f_{aH_a}, and R_a. The f_{aH_a} reduction due to ethanol addition involves an increase in the number of fused aromatic carbons. The R_a value of the chloroform-extractable material of soot obtained from the flame with ethanol is approximately seven rings for all the samples, whereas for the samples obtained from the neat flame the R_a value is between five and six rings. This result explains the low yield of chloroform-extractable material of soot, as well as the increment in the aromatic and carbon content obtained in the ethanol case, which also implies an increment in the size of the aromatic cluster.

The results presented here show that the average aromatic cluster of the soot precursor components found in an ethylene IDF is rapidly formed in the flame and remains almost constant through the exhaust; however, the nature of the aromatic cluster is affected by the presence of ethanol in the flame.

Acknowledgments

The authors thank the University of Antioquia for the support given to this project under the Sostenibilidad Program. A. Santamaría thanks Colciencias and the University of Antioquia for the Ph.D. scholarship.

References

[1] C.J. Carrell, T.J. Carrell, H.L. Carrell, J.P. Glusker, E. Abu-Shaqara, C. Cortez, R.G. Harvey, Carcinogenesis 15 (1994) 2931–2936.

[2] T.R. Barfknecht, Prog. Energy Combust. Sci. 9 (1983) 199–237.

[3] H. Burtscher, Aerosol Sci. 36 (2005) 896–932.

[4] C.A. Miller, W.P. Linak, Primary Particles Generated by the Combustion of Heavy Fuel Oil and Coal, Report No. EPA-600/R-02-093, National Risk Management Research Laboratory, 2002.

[5] A.F. Sarofim, J.S. Lighty, E.G. Eddings, Fuel Chem. Div. Prepr. 47 (2002) 618–621.

[6] B.S. Haynes, in: W. Bartok, A.F. Sarofim (Eds.), Fossil Fuel Combustion: A Source Book, Wiley, New York, 1991, p. 261.

[7] B.S. Haynes, H. Jander, H.G. Wagner, Proc. Combust. Inst. 17 (1979) 1365–1374.

[8] B.S. Haynes, H. Jander, H. Maetzing, H.G. Wagner, Combust. Flame 40 (1981) 101–103.

[9] V.I. Bushok, W. Stang, K.L. McNesby, Proc. Combust. Inst. 29 (2002) 2315–2323.

[10] M. Kasper, K. Sattler, K. Siegmann, U. Matter, H. Siegmann, J. Aerosol Sci. 30 (1999) 217–225.

[11] J.B. Mitchell, Combust. Flame 86 (1991) 179–184.

[12] J. Zang, C.M. Megaridis, Combust. Flame 105 (1996) 528–540.

[13] J.B. Howard, W.J. Kausch, Prog. Energy Combust. Sci. 6 (1980) 263–277.

[14] M.D. Rumminger, G.T. Linteris, Combust. Flame 128 (2002) 145–164.

[15] M.B. Colket, R.J. Hall, in: H. Bockhorn (Ed.), Soot Formation in Combustion, Springer-Verlag, Berlin, 1994, p. 417.

[16] C.Y. Choi, R.D. Reitz, Fuel 78 (1999) 1303–1317.

[17] F. Inal, S.M. Senkan, Combust. Sci. Technol. 174 (9) (2002) 1–19.

[18] T.N.S. Gupta, R.J. Santoro, Proc. Combust. Inst. 25 (1994) 585–592.

[19] P. Markatou, H. Wang, M. Frenklach, Combust. Flame 93 (1993) 467–482.

[20] J. Wu, K.H. Song, T.A. Litzinger, L.Y. Seong, R. Santoro, M. Linevsky, M. Colket, D. Liscinsky, Combust. Flame 144 (2006) 675–687.

[21] K.L. McNesby, A.W. Miziolek, T. Nguyen, F.C. Delucia, R. Skaggs, T.A. Litzinger, Combust. Flame 142 (2005) 413–427.

[22] K.H. Song, P. Nag, T.A. Litzinger, D.C. Haworth, Combust. Flame 135 (2003) 341–349.

[23] A. Alexiou, A. Williams, Combust. Flame 104 (1996) 51–65.

[24] G.W. Sidebotham, I. Glassman, Combust. Sci. Technol. 81 (1992) 207–219.

[25] G.W. Sidebotham, I. Glassman, Combust. Flame 90 (1992) 269–283.

[26] L.G. Blevins, N.Y. Yang, G.W. Mulholland, R.W. Davis, E.B. Steel, Prepr. Symp. Am. Chem. Soc. Div. Fuel Chem. 47 (2) (2002) 740–741.

[27] L.G. Blevins, R.A. Fletcher, B.A. Benner, E.B. Steel, G.W. Mulholland, Proc. Combust. Inst. 29 (2002) 2325–2333.

[28] K.C. Oh, U.D. Lee, H.D. Shin, E.J. Lee, Combust. Flame 140 (2005) 249–254.

[29] A. Santamaría, F. Mondragón, A. Molina, E.G. Eddings, N.D. Marsh, A.F. Sarofim, Combust. Flame 146 (2006) 52–62.

[30] A. Santamaría, F. Mondragón, W. Quiñónez, E.G. Eddings, A.F. Sarofim, Fuel 86 (2007) 1908–1917.

[31] J.K. Brown, W.R. Ladner, Fuel 39 (1960) 87–96.

[32] D.R. Clutter, L.Z. Petrakis, R.L. Stenger, R.K. Jensen, Anal. Chem. 44 (1972) 1395–1405.

[33] M.D. Guillen, C. Diaz, C.G. Blanco, Fuel Process. Technol. 58 (1998) 1–15.

[34] J.T. McKinnon, E. Meyer, J.B. Horward, Combust. Flame 105 (1996) 161–166.

[35] S. Di Stasio, A. Braun, Energy Fuels 20 (2006) 187–194.